J Comp Physiol A
DOI 10.1007/s00359-010-0576-7

ORIGINAL PAPER

A pair of motion-sensitive neurons in the locust encode approaches of a looming object

John R. Gray · Eric Blincow · R. Meldrum Robertson

Received: 9 May 2010 / Revised: 20 August 2010 / Accepted: 22 August 2010

Abstract Neurons in the locust visual system encode approaches of looming stimuli and are implicated in production of escape behaviours. The lobula giant movement detector (LGMD) and its postsynaptic partner, the descending contralateral movement detector (DCMD) compute characteristics of expanding edges across the locust eye during a loom and DCMD synapses onto motor elements associated with behaviour. We identified another descending interneuron within the locust ventral nerve cord. We named this neuron the late DCMD (LDCMD) as it responds later during an approach, with the firing rate peaking at about the time of collision. LDCMD produced lower amplitude, broader action potentials that were associated with an afterhyperpolarization, whereas DCMD action potentials showed a brief afterhyperpolarization often followed by an afterdepolarization. Within the mesothoracic ganglion, the primary LDCMD axon located adjacent to the DCMD axon, was thinner and lacked collateral projections to the lateral region of the neuropil. When compared with DCMD, LDCMD fired with fewer spikes during a loom and showed weaker habituation to repeated approaches. Coincidence of LDCMD and DCMD firing increased during object approach. Our findings indicate the presence of an additional motion-sensitive descending neuron in the locust that encodes temporally distinct properties of an approaching object.

Keywords Locust · Vision · Looming · DCMD · Collision detection

Introduction

Orientation within a complex environment often requires initiation and modulation of avoidance behaviours that are triggered by objects approaching on a direct collision course (i.e. looming). Modulation of these behaviours can be evoked by dynamic salient features of the stimulus as it approaches. Thus, behavioural strategies may change as a looming object draws nearer to the observer. Avoidance behaviours and looming detection have been studied in many systems ranging from humans (Vallis and McFadyen 2003; Vallis and McFadyen 2005; Gray and Regan 2006; Poljac et al. 2006) and other primates (Maier et al. 2004), gerbils (Ellard 2004; Maier et al. 2004), birds (Sun and Frost 1998; Cao et al. 2004), frogs (Yamamoto et al. 2003), fish (Gallagher and Northmore 2006; Preuss et al. 2006), crabs (Oliva et al. 2007) and many insects (Robertson and Johnson 1993; Jablonski and Strausfeld 2001; Verspui and Gray 2009; Yamawaki and Toh 2009). While many of these studies have provided much information on common mechanisms of looming detection and avoidance behaviour, less is known on how neural circuits detect dynamic stimulus properties to affect hierarchical behavioural responses. Likely, parallel visual pathways are needed to extract changing spatiotemporal stimulus properties associated with looming.

The locust is arguably one of the more extensively studied systems with respect to detection of looming

Electronic supplementary material The online version of this article (doi:10.1007/s00359-010-0576-7) contains supplementary material, which is available to authorized users.

J. R. Gray (✉) · E. Blincow
Department of Biology, University of Saskatchewan,
112 Science Place, Saskatoon, SK S7N 5E2, Canada
e-mail: jack.gray@usask.ca

R. M. Robertson
Department of Biology, Queen's University,
Kingston, ON K7L 3N6, Canada

Published online: 09 September 2010

stimuli. While escape and collision avoidance behaviours are associated with stereotypical leg (Pearson and O'Shea 1984) and wing kinematics (Robertson and Reye 1992; Santer et al. 2005) these behaviours can be variable (Gray et al. 2001), implying that the underlying neural circuitry can adapt to changing stimuli. One well-studied pair of motion-sensitive interneurons in the locust's visual system comprises the lobula giant movement detector (LGMD) and its postsynaptic partner, the descending contralateral movement detector (DCMD). During looming, integrated retinal inputs onto the LGMD evoke a characteristic increase in firing rate that can be measured as concurrent DCMD activity via a mixed chemical and electrical synapse (Rind 1984). The firing rate peaks after a defined retinal threshold angle is exceeded and, depending on the stimulus parameters, this peak occurs before or around the projected time of collision (Gabbiani et al. 2002, 2005; Krapp and Gabbiani 2005). Thus, these neurons are part of a well-defined pathway that provides information about the speed and size of the approaching object (Schlotterer 1977; Rind and Simmons 1997; Gabbiani et al. 1999; Guest and Gray 2006). DCMD, in turn, connects to thoracic interneurons and motor neurons associated with jumping and flight steering manoeuvres (Burrows and Rowell 1973; Simmons 1980; Robertson and Pearson 1983; Pearson and O'Shea 1984; Rogers et al. 2007). Thus, this pathway is implicated in the initiation and modulation of adaptive avoidance behaviours, such as jumping (Fotowat and Gabbiani 2007), gliding during flight (Santer et al. 2006) and flight steering (Gray et al. 2001).

While DCMD is implicated in initiation of flight steering, initiation of steering responses occur before an object reaches a threshold subtense angle that relates DCMD activity to looming stimulus properties (Gabbiani et al. 1999). Locusts initiate active steering 200 ms before collision (Gray et al. 2001; Matheson et al. 2004), yet DCMD fires at a relatively low rate at this time (<100 spikes/s, Guest and Gray 2006). These findings suggest that other neurons may be involved in collision avoidance. Recent studies suggest that looming stimuli also elicit a last ditch gliding behaviour in tethered flying locusts (Santer et al. 2005). A subsequent investigation further suggests that gliding is initiated when the DCMD firing rate exceeds 150 spikes/s, which may be mediated through summation of EPSPs in a postsynaptic flight steering motor neuron (Santer et al. 2006).

Rapid habituation of DCMD responses to repeated approaches of a looming object (Matheson et al. 2004; Gray 2005) likely occurs at synapses from retinotopic inputs onto the LGMD dendritic tree (Gray 2005). Whereas habituation is reduced in the gregarious phase of the locust's life history (Matheson et al. 2004) it is still present. Gregarious locusts in a swarm fly approximately 0.8–9.0 m apart at 3 m/s (Waloff 1972). In these conditions, it would be adaptive to detect and avoid conspecifics while flying. Rapid habituation of the LGMD/DCMD pathway could preclude production of effective avoidance strategies.

Given the timing difference between DCMD firing and active flight steering, rapid habituation of the DCMD pathway and temporally distinct avoidance behaviours (active steering vs. gliding), we set out to identify additional, putative motion-sensitive descending interneurons in the locust. We used a combination of intracellular and extracellular techniques to record from neurons in the ventral nerve cord and mesothoracic ganglia. This combination allowed us to unambiguously discriminate DCMD activity from that of other, currently unidentified neurons. We found an additional motion-sensitive neuron that projects within a similar region of the mesothoracic ganglion and responds to looming stimuli. Compared to DCMD activity, the response occurred later in the approach and produced a lower peak firing rate. Due to its distinct temporal firing properties, we named the neuron the late DCMD (LDCMD). Habituation trials show that LDCMD habituated significantly less than DCMD. We also observed that coincident firing between LDCMD and DCMD increased during the approach of a looming object.

Materials and methods

Animals

Adult male locusts (*Locusta migratora* L.) were selected at least 2 weeks past the imaginal moult from a crowded colony (30:26°C, 12 h:12 h light:dark cycle) maintained at Queen's University. Experiments were conducted at room temperature (approximately 23°C).

Preparation and neurophysiological recordings

We used a semi-intact preparation to expose the thoracic nervous system (Robertson and Pearson 1982). Following removal of the wings and legs, a dorsal midline incision was made from the anterior margin of the abdomen through the thorax. The locust was then pinned to a cork platform in the recording setup and the thoracic ganglia were exposed and mounted onto a metal plate. A chlorided silver wire was inserted into the abdomen and connected to ground.

For an extracellular monitor of DCMD activity we placed a suction electrode on the dorsal surface of the right connective of the ventral nerve cord immediately anterior to the mesothoracic ganglion (see Fig. 1). The signal was amplified using a Model P15 preamplifier (Grass Instruments, Inc., West Warwick, RI, USA), digitized using a

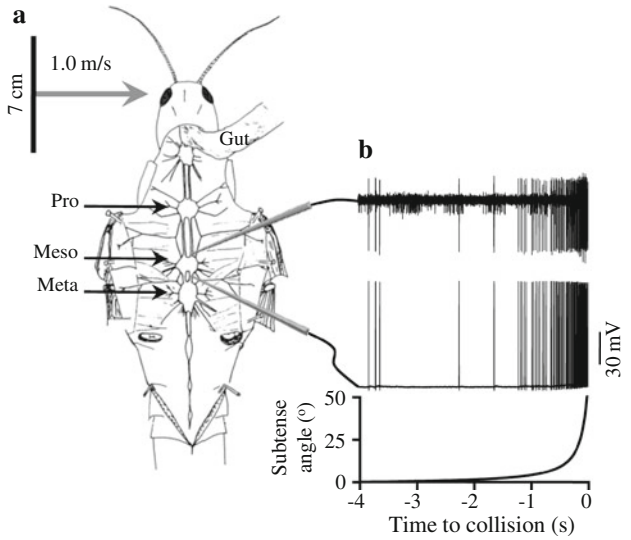

Fig. 1 Experimental setup and sample recordings. **a** A dorsal preparation was used to expose the thoracic ganglia. A suction electrode was placed on the connective anterior to the mesothoracic ganglion and an intracellular electrode was inserted into the posterior margin of the same ganglion. During recordings, the locust was presented with a computer-generated 7 cm diameter looming black disc approaching at 1.0 m/s. **b** Sample recording of DCMD activity from both electrodes and the subtense angle of the disc on the locust's eye aligned to the time of projected collision. Pro, meso, meta refer to the pro-, meso- and metathoracic ganglia, respectively

Digidata 1322A (Axon Instruments Inc. Union City, CA, USA) and recorded to a computer for off-line analysis. In this configuration, DCMD activity was clearly identifiable as the largest spike in the trace.

For intracellular recordings we used a borosilicate micropipette pulled to a resistance of 40–80 MΩ when filled with 1 M KAc. For a subset of preparations that were used for neuronal identification, the tip of the electrode was filled with 4% Lucifer Yellow and the rest of the electrode filled with 1 M LiCl. Intracellular signals were amplified using a Neuroprobe Model 1600 amplifier (A-M Systems, Everett, WA, USA) and digitized on a second channel of the Digidata acquisition system. Penetrations were made in the dorsomedial region of the right connective immediately posterior to the mesothoracic ganglion, typically 1 mm posterior to the extracellular recording site. Upon initial penetration, motion sensitivity was assessed by the experimenter waving a hand in the visual field of the ipsilateral or contralateral eye. DCMD activity was determined by observing time-aligned spiking with activity recorded from the suction electrode. Conversely, non-time-aligned spiking activity suggested the presence of another motion-sensitive neuron, which was then tested for responses to looming stimuli.

For preparations using Lucifer Yellow-filled electrodes, we applied a hyperpolarizing current (8–15 nA) for 10–30 min following the completion of a stimulus regime. After removal of the electrode, these preparations were allowed to remain for 15–30 min to allow the dye to diffuse within the cell. The thoracic ganglia (prothoracic, mesothoracic and metathoracic) were then removed and processed for fluorescence microscopy. The tissue was fixed in 4% paraformaldehyde at 4°C overnight, dehydrated in an ascending ethyl alcohol series, cleared with methyl salicylate, and temporarily mounted onto a well slide for visualization. Whole mounts were imaged using a fluorescence microscope (High Performance CCD Cool SNAP ES Roper Scientific mounted on a Olympus BX50WI) equipped with a FITC filter. Ganglia were imaged with either a 10× or 40× objective lens using SlideBook 4 (Intelligent Image Innovations) software and digitized images were stored on a computer.

Visual stimuli

Creation of visual stimuli was similar to a technique reported previously (Money et al. 2006). Looming stimuli were emulated by generating a black disc against a white background (contrast ratio = 0.92) using macromedia Flash MX 2004 software (Macromedia, Inc.) and displayed using a Sharp XG-C55X LCD projector (Sharp Electronics Inc.) projecting onto a rear projection screen. Each pixel of the projected image subtended <1° of the locust's visual field, which is below the spatial resolution of each ommatidium (Horridge 1978). We rendered the frames of the stimuli at 100 fps (frames/s), which is above the flicker fusion frequency of the locust eye (Miall 1978), using an ATI Radeon 256 MB video card built into the dedicated visual stimulus generation computer. The projection screen was placed 10 cm from the locust's left eye perpendicular to the long body axis and the centre of the disc was centred on the eye. The first image (frame) of the disc subtended <1° of the locust's visual field and approached at 1 m/s, ending with a final subtense angle of 50°. The disc disappeared immediately after the last frame.

Brief audio signals, <10 ms, were embedded within the first and last frame of the Macromedia file and used to mark the start and end of approach, respectively. These signals were connected to a third channel of the Digidata system and used to time align the stimulus to the neural recordings.

For most preparations, we waited at least 5 min between approaches to avoid confounding effects of habituation that is known to exist with the locust DCMD (Matheson et al. 2004; Gray 2005). For a subset of animals, we specifically tested for habituation by repeatedly presenting a looming stimulus 20–50 times with each approach starting immediately following the end of the previous approach.

Data analysis

Spike times from raw extracellular and intracellular records as well as the times of the embedded stimulus pulses were extracted using a threshold detection function in Offline Sorter (Plexon Inc., Dallas, TX, USA). The time of projected collision (TOC) was determined by calculating the amount of time taken by the disc to travel the final 10 cm to the locust's eye and adding this to the time of the second stimulus pulse, which represented the last frame of the approach. Using Neuroexplorer spike train analysis software (NEX technologies, Littleton, MA, USA), spike times were aligned to TOC, which was used as the reference event to generate peristimulus time histograms (PSTH). These histograms were smoothed with a 50 ms Gaussian filter to estimate changes in the firing rate during approaches.

Firing parameters that described the response profile of DCMD (Supplementary Figure 1) included peak firing rate, time of peak firing, peak width at ½ maximum firing, the number of spikes and the firing rate at $t = -0.2$ s, which is the time associated with the initiation of collision avoidance behaviour in flying locusts (Gray et al. 2001). For habituation trials, we plotted these parameters for each approach.

Correlation analysis was used to test for individual firing patterns of DCMD and LDCMD, coincident firing between the two neurons and coincident dynamics during an approach (see text for details).

Statistical methods

We used SigmaStat 3.0 (Systat Software Inc., Richmond, CA, USA) to compare firing parameters between neurons. Putative differences between DCMD and LDCMD firing parameters during single approaches were assessed with a Student's t test, or a Mann–Whitney rank sum test for non-parametric data. Putative differences in habituation of firing parameters during repeated approaches were assessed using a paired t test, or a Wilcoxon signed rank test for non-parametric data. Resulting statistics are described in appropriate sections of "Results". Significance was assessed at $P < 0.05$. Normally distributed data are presented as the mean ± standard deviation. Data that did not pass tests for normality or equal variance are presented as the median and the range.

Results

Physiological and morphological distinction of LDCMD and DCMD

In eight preparations we were able to discriminate LDCMD and DCMD activity in extracellular traces and record from each neuron with different penetrations using sharp electrodes. LDCMD and DCMD produced robust spiking during non-specific contralateral visual motion initially following penetration with sharp electrodes. Neither of the neurons responded to ipsilateral motion (data not shown). LDCMD and DCMD action potentials differed with respect to temporal and amplitude properties. LDCMD evoked significantly lower amplitude spikes ($U = 48.0$, $P = 0.001$) that were of significantly longer duration ($t_{12} = 2.34$, $P = 0.037$, Fig. 2a). The median LDCMD spike amplitude was 82.4 mV (range 78.5–95.3 mV), whereas the median DCMD spike amplitude was 100.2 mV (range 93.0–103.5 mV). The mean width of the spike at half the peak amplitude was 0.367 ± 0.044 ms for LDCMD and 0.317 ± 0.037 ms for DCMD. We observed longer conduction delays in LDCMD and were able to calculate conduction velocities based on an inter-electrode distance of 1 mm (see "Methods"). LDCMD conduction velocity (2.0 ± 0.2 m/s) was significantly lower than that of DCMD (2.6 ± 0.3 m/s, Fig. 2b). While both LDCMD and DCMD hyperpolarized at the end of each action potential (Fig. 2a) we observed slower membrane potential changes that occurred on a longer time scale. From intracellular records, all preparations ($n = 8$) showed a clear afterhyperpolarization following individual LDCMD spikes, whereas DCMD spikes displayed an afterdepolarization in 8 out of 13 preparations (arrows in Fig. 2c). These afterpotentials resulted in slower hyperpolarization and depolarization of the LDCMD and DCMD membrane potential, respectively, during peak activity associated with a looming stimulus.

Representative Lucifer yellow fills from two different preparations showed that the mesothoracic projection of the LDCMD axon was thinner than that of DCMD and showed none of the prominent collateral projections to the medial, lateral and ventral regions of the neuropil typical of DCMD (Fig. 3a). Smaller collateral projections of the LDCMD were confined to the medial region of the ganglion and extended primarily ventrally. These observations were consistent in all successful fills ($n = 5$ for each neuron).

Raster plots pooled from 70 approaches to 29 locusts (Fig. 3b) showed that LDCMD consistently fired later during the approach and generated fewer spikes. Mean responses (Fig. 3b, bottom) showed that peak LDCMD activity occured later than that of DCMD. Specifically, LDCMD generated fewer spikes (Figs. 2, 4) that resulted in a lower peak firing rate (Fig. 4a, $t_{134} = 9.18$, $P < 0.001$) that occurred later in the response (Fig. 4b, $U = 640.5$, $P < 0.001$). LDCMD also produced a shorter response (Fig. 4c, $U = 3949$, $P < 0.001$) and lower firing rate at a behaviourally relevant time point during the approach (Fig. 4d, $U = 664$, $P < 0.001$). These differences coincided with fewer spikes from LDCMD during an approach (Fig. 4e, $U = 195.5$, $P < 0.001$).

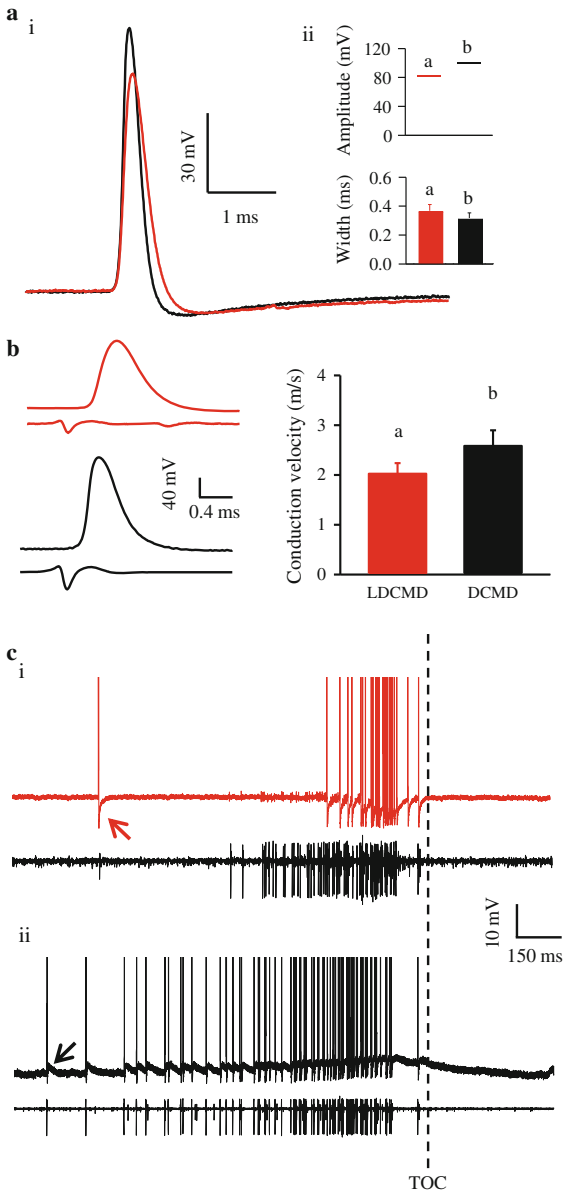

Fig. 2 LDCMD and DCMD action potential properties. **a** *i* Overlay of a typical action potential from LDCMD (*red*) and DCMD (*black*). *ii* Comparison of LDCMD (*red*) and DCMD (*black*) action potential amplitude and width ($n = 8$). **b** Intracellular (*top trace*) and extracellular (*bottom trace*) recordings of LDCMD (*red*) and DCMD (*black*) from the same preparation and comparison of conduction velocities ($n = 8$). **c** Recordings from two different preparations showing responses to a loom. The *red arrow* indicates a distinct LDCMD afterhyperpolarization, whereas the *black arrow* indicates a DCMD afterdepolarization. The bottom traces in *i* and *ii* are extracellular records from the nerve cord showing DCMD activity. TOC is the time of projected collision. Data in the top graph of **a** *ii* are plotted as box plots including the median value and interquartile range. The narrow range of data values is represented by indistinguishably small interquartile ranges. The data in bottom plot and in *b* are plotted as the mean ± SD. Different letters above each box or bar indicate significant differences. See text for details. The peaks of the action potentials from intracellular recordings in **c** *i* and *ii* were clipped to highlight afterhyperpolarization and afterdepolarization of the membrane potential

Habituation of DCMD and LDCMD looming responses

Descending contralateral movement detector (DCMD) looming responses fully habituated to repeated presentations of a disc, typically after 10–15 approaches (Fig. 5). In the fully habituated state, DCMD no longer responded to looming stimuli approaching within the same visual field of the eye. Whereas LDCMD displayed habituation, the effect was milder such that a decreased, yet clear, response was maintained for all approaches.

To compare LDCMD and DCMD response profiles during repeated approaches we plotted peristimulus time histograms for each approach in a series. Supplementary Figure 2 shows LDCMD and DCMD responses from a single locust. The first response showed clear distinctions between LDCMD and DCMD profiles that were consistent with mean responses to single approaches (Fig. 3b). Whereas the profiles for each neuron changed during repeated approaches, the effect was more dramatic for DCMD and there was no discernable DCMD response after the tenth approach. Conversely, after moderate attenuation within the first three approaches, LDCMD activity continued to generate a distinct and consistent peak firing rate throughout all 20 approaches. These findings were consistent in all preparations ($n = 8$ locusts) and, therefore, we were able to examine the quantitative properties of the responses during habituation (Fig. 6). Generally, we found clear differences in the extent of habituation between LDCMD and DCMD. We used a paired t test (Wilcoxon signed rank test for nonparametric data) to assess putative differences for each approach in a series. Habituation plots were significantly different for the peak firing rate (Fig. 6a, $t_{48} = 6.94$, $P < 0.001$), time of peak firing (Fig. 6b, $t_{36} = -2.06$, $P = 0.046$), peak width at half max (Fig. 6c, $Z = -2.17$, $P = 0.03$) and the number of spikes (Fig. 6e, $Z = -3.03$, $P = 0.002$). There was, however, no difference in habituation of the firing rate 200 ms before collision (Fig. 6d). It should be noted that the habituated DCMD peak firing rates (approximately 40 spikes/s) are a result of the Gaussian filter method and does not reflect the actual spontaneous firing rate. Nevertheless, this filter is a valid technique for estimating DCMD firing properties (Gabbiani et al. 1999; Matheson et al. 2004; Gray 2005).

To compare the relative extent of habituation between DCMD and LDCMD we normalized each firing parameter measured by dividing the value during the last approach to that of the first approach (Supplementary Figure 3). These normalized data showed a milder habituation in LDCMD. Following habituation, the LDCMD had a relatively higher peak firing rate ($t_{14} = -3.72$, $P = 0.002$), longer response ($t_{14} = -7.33$, $P < 0.001$), higher firing rate 200 ms before collision ($U = 64$, $P = 0.013$) and generated relatively more spikes ($U = 64$, $P < 0.001$). Linear regressions for

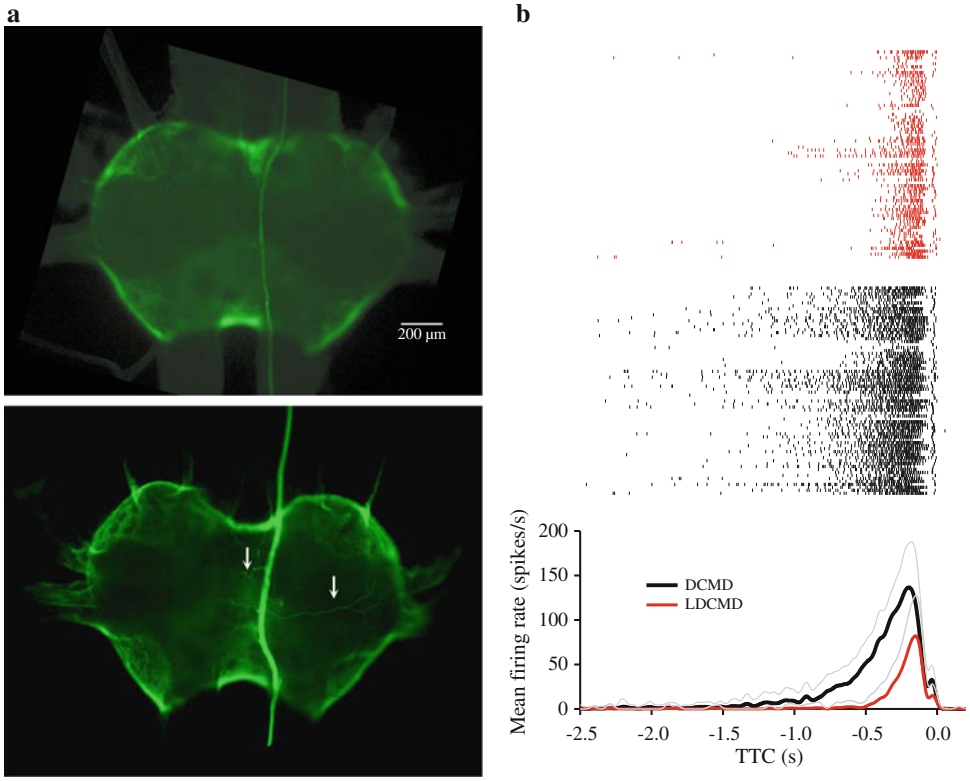

Fig. 3 Mesothoracic projections and response profiles of LDCMD and DCMD. **a** Whole mounts of mesothoracic ganglia from different preparations showing Lucifer yellow fills of the LDCMD (*top*) and DCMD (*bottom*) axon. *Arrows* indicate collateral branches of the primary DCMD axon. Anterior is toward the top of each image. **b** Top rasters show individual responses of LDCMD (*red*) and DCMD (*black*) to 70 approaches (pooled from $n = 29$ locusts). Mean peristimulus time histograms (*bottom plot*) reveal distinct LDCMD (*red*) and DCMD (*black*) responses to looming. *Grey lines* represent the positive standard deviation from all approaches. The small peaks in the histograms that occur near the time of projected collision (TTC = 0 s) are the off responses of each neuron when the disc disappeared. Approaches to the same animal were separated by an interstimulus interval of 5 min to avoid habituation

the time of peak firing showed no effect of presentation number for either neuron (DCMD $r^2 = 0.02$; LDCMD $r^2 = 0.005$). Therefore, relative habituation could not be compared for this parameter. Together, these data demonstrate that LDCMD was more resistant to habituation than DCMD.

Spiking properties and correlated LDCMD–DCMD firing

To compare temporal spiking patterns of LDCMD and DCMD we calculated the autocorrelograms for each neuron (Fig. 7). Other than a slow decay in the spiking probability, tapering off 20 ms either side of a spike, there were no discernible patterns in LDCMD spike trains during responses to looming (Fig. 7, top). Conversely, DCMD spike trains showed consistent modulation with a period of 16 ms (Fig. 7, middle). This difference in spiking properties was reflected in the power spectral densities of each neuron (Supplementary Figure 4). Coincident firing of two extracellularly recorded spike trains could reflect synaptic input from one neuron to the other or common presynaptic input to both (Ostojic et al. 2009). To measure putative coincident firing of LDCMD and DCMD we generated a crosscorrelogram for LDCMD with DCMD as the reference spike (Fig. 7, bottom) and tested the resulting distribution to a theoretical Poisson distribution that would be generated from independent spike trains. The Poisson distribution was calculated as the mean of all possible shifts from a shift predictor used to remove stimulus-induced covariation of the firing rates of each neuron (Smith and Kohn 2008). The raw crosscorrelogram was not significantly different from a predicted Poisson distribution ($\chi^2_{16896} = 17038.33$, $P = 0.219$), suggesting that LDCMD and DCMD firing were not independent. The corrected crosscorrelogram (raw-shift predictor) showed a clear peak at approximately 7 ms, suggesting that a LDCMD spike occurred 7 ms after a DCMD spike.

A putative stimulus-induced shift in the raw crosscorrelation suggests that the relationship between LDCMD and DCMD firing changed during the approach of a looming stimulus. Therefore, we created a joint peristimulus

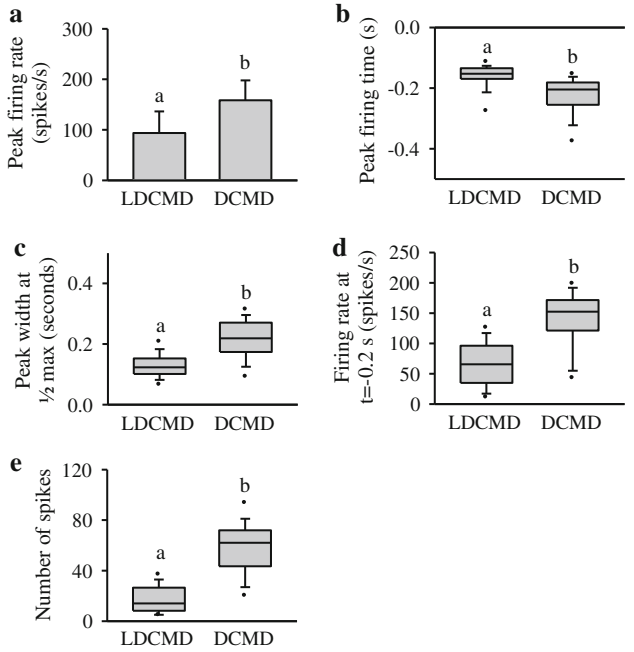

Fig. 4 Distinct LDCMD firing properties. Parametric data in **a** (*bar chart*) were compared with a student's *t* test, whereas non-parametric data in **b–e** (box plots) were compared with a Mann–Whitney rank sum test. *Error bars* in a represent standard deviation. *Boxes* indicate interquartile range and median value, *whiskers* indicate the 5 and 95% confidence levels and *dots* indicate range. Different letters above each *bar* or *box* indicate significant differences. $n = 70$ approaches to 29 locusts

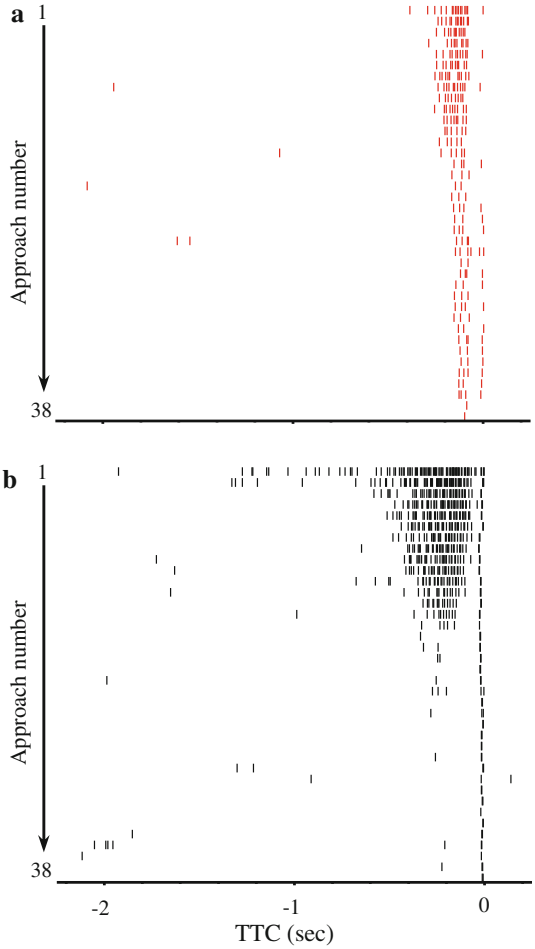

Fig. 5 Sample raster plots of LDCMD (**a**) and DCMD (**b**) spike times in response to repeated approaches. All data are from presentations to a single locust. Each of the 38 rows of rasters represents the response to a single approach. Each successive approach after the first began immediately following the end of the previous approach. Spike times near the time of projected collision (TTC = 0) represent the off response of each neuron as the disc disappeared from the screen

time histogram (JPSTH), with the time of projected collision as the reference event, to determine if there was a change in the correlation of firing between the two neurons during an approach (Fig. 8). As with the crosscorrelation, the JPSTH correlation matrix was corrected to remove firing covariation due to stimulation. The corrected matrix was obtained by subtracting, bin by bin, the shift predictor from the raw matrix and then dividing, again bin by bin, by the product of the individual neurons' PSTH standard deviations. The corrected matrix counts thus represent correlation coefficients ranging from −1 to 1. The matrix differed from that of a random distribution as assessed using the "surprise" method of calculating a matrix represented by binary values of coincidence (see Supplementary Figure 5, Aertsen et al. 1989). The coincidence (diagonal) histogram in Fig. 8 shows a change in firing correlation during stimulus approach. Coincidence values were consistently positive starting 514 ms before collision (black arrow) and remained high starting 200 ms before collision (red arrow). A maximum coincidence of 0.615 (not shown) occurred 134 ms before collision. These data demonstrate that LDCMD and DCMD firing become more strongly correlated during object approach, remaining high at a time when flight steering behaviours are initiated in flying locusts (200 ms before collision, Gray et al. 2001).

Discussion

This paper identifies an additional motion-sensitive descending interneuron (LDCMD) in the locust that responds to looming stimuli. The main branch of the LDCMD axon lies adjacent to the DCMD axon within the same axon tract of the mesothoracic ganglion and meso-metathoracic connective. Compared to DCMD, LDCMD produced lower amplitude, longer lasting spikes that were conducted more slowly along the axon. Moreover, an afterhyperpolarization in LDCMD led to hyperpolarization of the membrane potential during a looming response, whereas the DCMD membrane potential, following a brief afterhyperpolarization, depolarized as a result of summed afterdepolarizations associated with each action potential. Further experiments are needed to determine why DCMD

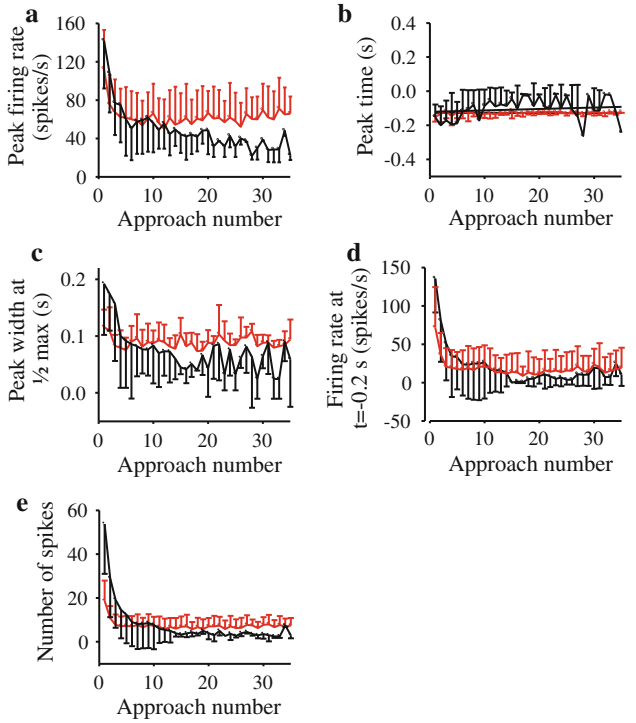

Fig. 6 Comparative habituation of LDCMD (*red*) and DCMD (*black*) firing parameters. Values for the peak firing rate (**a**), peak width at half max (**c**), the firing rate at $t = -0.2$ s (**d**) and the number of spikes (**e**) were initially higher during DCMD responses to looming. However, following habituation, looming evoked a stronger response in LDCMD. The time of peak LDCMD firing (**b**) was initially later than that of DCMD but occurred earlier and was less variable following 10 approaches. $n = 8$ locusts

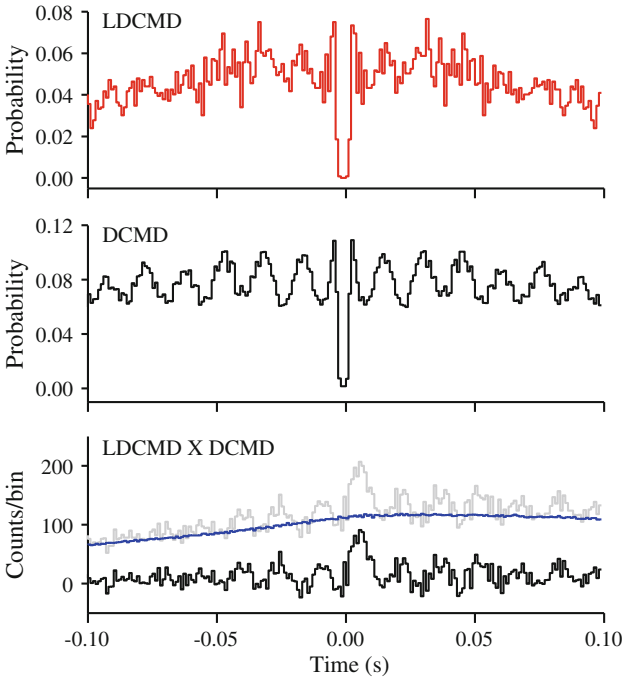

Fig. 7 Firing dynamics of LDCMD and DCMD and correlated spiking. The LDCMD (*top*, *red*) and DCMD (*middle*, *black*) plots are autocorrelations for each neuron. The bottom plot shows the crosscorrelation between LDCMD and DCMD during single approaches of a looming disc. Data were shifted by 1 trail to remove potential correlation due to co-stimulation (see text for details). The *grey line* represents the raw crosscorrelation. The *blue line* is the shift predictor and the *black line* is the corrected crosscorrelation (raw-predictor). After correction, there remains a clear peak at 7 ms (i.e. there is a probability of a LDCMD spike occurring 7 ms after a DCMD spike). Bin width = 1 ms

afterdepolarization was not observed in all preparations. Like DCMD, LDCMD responded to looming objects approaching the eye contralateral to the thoracic axon and the firing rate increased during approach, peaking before the time of projected collision. LDCMD was distinct from DCMD in that the looming response began later in the approach, the peak firing rate was lower and occurred closer to the time of collision. Moreover, LDCMD habituated less than DCMD during repeated approaches. Correlation analysis showed that LDCMD and DCMD spiking were correlated during presentation of a looming stimulus and the strength of this correlation increased during a time when both neurons were responding to looming.

During intracellular LDCMD recording sessions, the resting membrane potential remained stable for at least 20–30 min, long enough to carry out the experiments and inject a sufficient amount of Lucifer Yellow to visualize projections within the mesothoracic ganglion. However, this amount of time was not sufficient to inject enough dye within this small diameter axon to completely fill a neuron that possibly extends from the head to the metathoracic ganglion. Complete morphological characterization of locust descending interneurons typically involves penetrations in the brain (Rind 1984) or a combination of filling techniques (Griss and Rowell 1986). Therefore, we cannot determine, unambiguously, that we recorded from the same neuron in each preparation. However, successful fills ($n = 5$) showed that each putative LDCMD axon projected within the same region of the mesothoracic ganglion and that finer branches consistently terminated in the same medio-ventral region of the neuropil. Moreover, we observed consistent LDCMD looming responses that were distinct from those of DCMD and equally variable. These responses were observed in intracellular and extracellular records, the latter of which is used routinely to identify DCMD activity. While full characterization requires a complete anatomical description, the intent of this study was to test the hypothesis that other looming sensitive neurons project within the thoracic ganglia. Future work is needed to more completely characterize detailed LDCMD morphology.

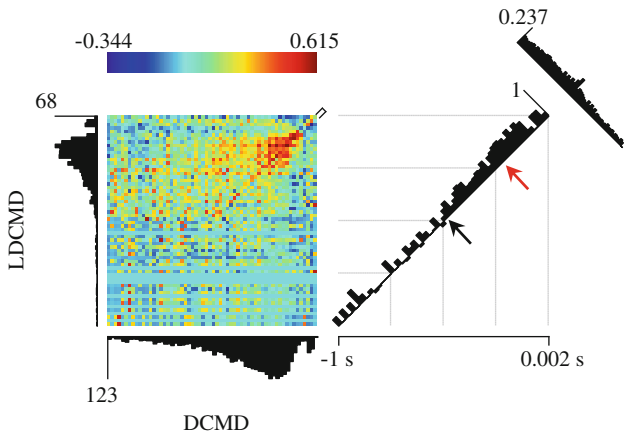

Fig. 8 Joint peristimulus time histogram (JPSTH) showing stimulus-induced coincidence of LDCMD and DCMD firing during responses to looming stimuli. Data were aligned to TOC and placed into 16.7 ms bins. The LDCMD (*left*) and DCMD (*bottom*) PSTHs were used to generate the corrected correlation matrix (see text for details). The *colour scale bar* defines the range of the correlation coefficients presented in each pixel of the correlation matrix. The diagonal, coincidence histogram, describes the coincidence of LDCMD and DCMD firing during an approach. The *black arrow* indicates the time at which the coincidence consistently rises above 0 ($t = -514$ ms) and the *red arrow* indicates 200 ms before collision. The non-stimulus-related crosscorrelation between LDCMD and DCMD is shown perpendicular to the coincidence histogram. The small secondary peaks at the end of each peristimulus time histogram and the diagonal coincidence histogram are produced by the off responses of each neuron when the disc disappeared from the screen. Data were pooled from 4509 DCMD spikes and 1293 LDCMD spikes from 70 single approaches to 29 locusts

A distinct looming-sensitive neuron in the locust

While many descending locust interneurons other than DCMD respond to visual stimuli, only one, the descending ipsilateral motion detector (DIMD), is known to respond to looming and it is implicated in the initiation of a jumping response (Burrows and Rowell 1973). However, DIMD carries information along the side of the body ipsilateral to the stimulated eye, whereas LDCMD reports contralateral visual motion. Therefore, the two are distinct neurons.

In *Schistocerca gregaria*, activity from multiple, multimodal S-units can be recorded extracellularly in the ventral nerve cord and these are sensitive to contralateral visual stimuli (Catton 1980, 1982, 1988; Rowell and Pearson 1983). While S-units are clearly distinct from DCMD (Catton 1988), further experiments are needed to determine if this distinction applies to LDCMD as well.

LDCMD could be the DNC neuron reported in earlier studies (Griss and Rowell 1986; Rowell and Reichert 1986). The DNC cell body lies along the midline of the protocerebrum and the main axon descends contralaterally. Within the neck connective, the DNC axon lies adjacent and lateral to the DCMD axon (see Fig. 7 in Griss and Rowell (1986)), which is the same relative position of the LDCMD within the meso-metathoracic connective. However, DNC is sensitive to large field visual motion associated with the orientation of the locust in space and thus is presumed to function as a deviation detector via inputs primarily from the ocelli (Rowell and Reichert 1986). While our experimental protocol cannot rule out ocellar input in shaping LDCMD activity, extensive studies on the LGMD clearly demonstrate that input from multiple ommatidia of the compound eye is necessary to code expanding edges from small field stimuli (Rind and Bramwell 1996; Gabbiani et al. 2002). Therefore, our data suggest that DNC and LDCMD are distinct neurons. Other described attitude deviation detection neurons receive input from the ipsilateral visual field (Rowell and Reichert 1986) and thus are likely not involved in the responses we observed here. Taken together, our data suggest that LDCMD is a distinct descending visual neuron that encodes object approaches. This presumption notwithstanding, future experiments are needed to fully characterize LDCMD motion sensitivity and to test the hypothesis that it is preferentially sensitive to looming.

Putative LDCMD connectivity

While we were not able to identify neurons presynaptic to LDCMD, responses to looming suggest that input comes from retinal networks that also drive LGMD, and, subsequently, DCMD. However, our observations of LDCMD firing times during an approach (Fig. 4) and relatively weak habituation (Fig. 6) imply that LDCMD may not receive the same direct input as DCMD (i.e. from LGMD, Rind 1984). It remains to be tested, however, if LGMD activates LDCMD directly through a rectifying synapse or indirectly via another interneuron and if a slower LDCMD conduction velocity (Fig. 2) could account for the 7 ms peak observed in the DCMD/LDCMD crosscorrelogram (Fig. 7) and a later peak firing time. These possibilities were, however, beyond the scope of the experiments described here. Future experiments could also test the possibility that DCMD itself synapses onto LDCMD, which would be consistent with a shifted peak in the crosscorrelogram.

It is also possible that LDCMD receives input via LGMD2, which also responds to looming dark objects (Simmons and Rind 1997). LGMD2 responses to various types of visual motion differ to some degree (Simmons and Rind 1997), which could be reflected in the differing responses between DCMD and LDCMD. Moreover, LGMD2 does not synapse with DCMD and its postsynaptic partners are not known (Simmons and Rind 1997). However, like LGMD1, LGMD2 habituates quickly in response

to repeated stimulation (Rind 1987) suggesting that LDCMD does not receive input from LGMD2.

Two other groups of motion-sensitive neurons in the locust optic lobe (Rind 1987) likely do not drive LDCMD looming responses. These groups receive either binocular or monocular ipsilateral retinal input (Rind 1987). Here, we show that LDCMD receives monocular visual information from the eye contralateral to its axonal projection.

In our study, we did not identify postsynaptic targets of LDCMD. However, morphological data showed relatively little collateral branching within the mesothoracic ganglia. The ventromedial connections we observed suggest that LDCMD synapses onto thoracic interneurons or commissural projections of flight motoneurons (Burrows 1996). In contrast, lateral DCMD projections reflect monosynaptic connections to interneurons and motoneurons associated with flight and jumping (Burrows and Rowell 1973; Simmons 1980; Robertson and Pearson 1983). Further experiments are needed to identify neurons presynaptic and postsynaptic to LDCMD and test the hypotheses that this neuron: (1) is either driven by a distinct motion-sensitive network within the optic lobe neuropils or is less sensitive to the same network that drives the LGMD-DCMD pathway and (2) drives motor elements associated with a collision avoidance behaviour.

Significance of an additional motion-sensitive pathway

Peak DCMD firing has been implicated in providing a relevant cue for impending collision and thus generation of collision avoidance behaviours (Hatsopoulos et al. 1995). More recently, peak firing (Gabbiani et al. 1999) and jumping in response to looming stimuli (Fotowat and Gabbiani 2007) have been related to a delay that occurs after a threshold subtense angle has been reached during an approach. However, at approach speeds of 3 m/s, changes in wing kinematics associated with collision avoidance begin 200 ms before collision (Gray et al. 2001), which is earlier than the time that the disc (10 cm diameter) reached an angular threshold of 15°–40° (47–127 ms before collision, respectively, calculation based on Gabbiani et al. 1999). More recent findings showed that, for comparable stimulus characteristics, locusts generate last ditch gliding responses within the last 50 ms of an approach (Santer et al. 2005) and may be driven by DCMD firing rates >150 spikes/s (Santer et al. 2006). However, there is no information on the timing of glide onset at the approach speed we used (1 m/s). Extrapolating from Fig. 4 of (Santer et al. 2005) and assuming a linear relationship, an approach at 1 m/s would initiate a glide 45 ms before collision, with a range of approximately ±75–100 ms. The time of LDCMD peak firing was 160 ms (range 320–30 ms) before collision and DCMD peak time was 230 ms (range 690–140 ms) before collision. Thus, peak LDCMD activity occurs in a time window that overlaps with the initiation of a glide. While LDCMD generates fewer spikes and a lower peak firing rate relative to DCMD during an approach, this weaker input to putative downstream motor elements may be sufficient to initiate a less complicated response, such as a glide. In gold fish, a single M-neuron spike has been correlated with a C-start response evoked by looming visual stimuli (Preuss et al. 2006). It would be useful to test the hypothesis that relatively weak LDCMD activity serves as a signal to evoke a last ditch evasive behaviour (i.e. gliding).

One of the more intriguing findings from the data reported here is that the coincidence of LDCMD and DCMD firing increases during looming, becomes consistently positive 514 ms before collision and reaches an upper range at a behaviourally relevant time (200 ms before collision, Fig. 8). Experiments are needed to identify LDCMD's presynaptic inputs and postsynaptic targets and further test if coincident firing with DCMD is involved in initiation of earlier, more coordinated flight steering behaviours. Such experiments could also test for stability of coincident firing during DCMD habituation to address the challenge of maintaining sensitivity to looming while flying in a chaotic swarm containing many looming objects, such as conspecifics or predators.

Acknowledgments We thank T. G. A. Money for providing valuable comments on an earlier version of the manuscript. This work was supported by grants from the Natural Science and Engineering Research Council of Canada (NSERC) to J. R. Gray and R. M. Robertson as well as a University of Saskatchewan Graduate Teaching Fellowship to E. Blincow.

References

Aertsen AM, Gerstein GL, Habib MK, Palm G (1989) Dynamics of neuronal firing correlation: Modulation of "Effective connectivity". J Neurophysiol 61:900–917

Burrows M (1996) The neurobiology of an insect brain. Oxford University Press, Oxford

Burrows M, Rowell CHF (1973) Connections between descending visual interneurons and metathoracic motoneurons in the locust. J Comp Physiol A 85:221–234

Cao P, Gu Y, Wang SR (2004) Visual neurons in the pigeon brain encode the acceleration of stimulus motion. J Neurosci 24:7690–7698

Catton WT (1980) Tonic effects of stationary luminous slits on the discharge rates of some locust visual interneurones. J Insect Physiol 26:373–379

Catton WT (1982) The effects of stimulus area and intensity on the on/off ratio of some locust visual interneurones. J Insect Physiol 28:285–291

Catton WT (1988) Discharge patterns of locust visual interneurones. Physiol Entomol 13:147–152

Ellard CG (2004) Visually guided locomotion in the gerbil: a comparison of open- and closed-loop control. Behav Brain Res 149:41–48

Fotowat H, Gabbiani F (2007) Relationship between the phases of sensory and motor activity during a looming-evoked multistage escape behavior. J Neurosci 27:10047–10059

Gabbiani F, Krapp HG, Laurent G (1999) Computation of object approach by a wide-field motion-sensitive neuron. J Neurosci 19:1122–1141

Gabbiani F, Krapp HG, Koch C, Laurent G (2002) Multiplicative computation in a visual neuron sensitive to looming. Nature 420:320–324

Gabbiani F, Cohen I, Laurent G (2005) Time-dependent activation of feed-forward inhibition in a looming-sensitive neuron. J Neurophysiol 94:2150–2161

Gallagher SP, Northmore DPM (2006) Responses of the teleostean nucleus isthmi to looming objects and other moving stimuli. Vis Neurosci 23:209–219

Gray JR (2005) Habituated visual neurons in locusts remain sensitive to novel looming objects. J Exp Biol 208:2515–2532

Gray R, Regan DM (2006) Unconfounding the direction of motion in depth, time to passage and rotation rate of an approaching object. Vis Res 46:2388–2402

Gray JR, Lee JK, Robertson RM (2001) Activity of descending contralateral movement detector neurons and collision avoidance behaviour in response to head-on visual stimuli in locusts. J Comp Physiol A 187:115–129

Griss C, Rowell CHF (1986) Three descending interneurons reporting deviation from course in the locust. I. Anatomy. J Comp Physiol A 158:765–774

Guest BB, Gray JR (2006) Responses of a looming-sensitive neuron to compound and paired object approaches. J Neurophysiol 95:1428–1441

Hatsopoulos N, Gabbiani F, Laurent G (1995) Elementary computation of object approach by a wide-field visual neuron. Science 270:1000–1003

Horridge GA (1978) The separation of visual axes in apposition compound eyes. Phil Trans R Soc (Lond) B 285:1–59

Jablonski PG, Strausfeld NJ (2001) Exploitation of an ancient escape circuit by an avian predator: relationships between taxon-specific prey escape circuits and the sensitivity to visual cues from the predator. Brain Behav Evol 58:218–240

Krapp HG, Gabbiani F (2005) Spatial distribution of inputs and local receptive field properties of a wide-field, looming sensitive neuron. J Neurophysiol 93:2240–2253

Maier JX, Neuhoff JG, Logothetis NK, Ghazanfar AA (2004) Multisensory integration of looming signals by rhesus monkeys. Neuron 43:177–181

Matheson T, Rogers SM, Krapp HG (2004) Plasticity in the visual system is correlated with a change in lifestyle of solitarious and gregarious locusts. J Neurophysiol 91:1–12

Miall RC (1978) The flicker fusion frequencies of six laboratory insects, and the response of the compound eye to mains fluorescent 'ripple'. Physiol Entomol 3:99–106

Money T, DeCarlo C, Robertson R (2006) Temperature-sensitive gating in a descending visual interneuron, DCMD. J Comp Physiol A 192:915–925

Oliva D, Medan V, Tomsic D (2007) Escape behavior and neuronal responses to looming stimuli in the crab *Chasmagnathus granulatus* (decapoda: Grapsidae). J Exp Biol 210:865–880

Ostojic S, Brunel N, Hakim V (2009) How connectivity, background activity, and synaptic properties shape the cross-correlation between spike trains. J Neurosci 29:10234–10253

Pearson KG, O'Shea M (1984) Escape behavior of the locust. The jump and its initiation by visual stimuli. In: Eaton RC (ed) Neural mechanisms of startle behavior. Plenum Press, New York, pp 163–178

Poljac E, Neggers B, Berg AV (2006) Collision judgment of objects approaching the head. Exp Brain Res 171:35–46

Preuss T, Osei-Bonsu PE, Weiss SA, Wang C, Faber DS (2006) Neural representation of object approach in a decision-making motor circuit. J Neurosci 26:3454–3464

Rind FC (1984) A chemical synapse between two motion detecting neurones in the locust brain. J Exp Biol 110:143–167

Rind FC (1987) Non-directional, movement sensitive neurones of the locust optic lobe. J Comp Physiol A 161:477–494

Rind FC, Bramwell DI (1996) Neural network based on the input organization of an identified neuron signaling impending collision. J Neurophysiol 75:967–985

Rind FC, Simmons PJ (1997) Signaling of object approach by the DCMD neuron of the locust. J Neurophysiol 77:1029–1033

Robertson RM, Johnson AG (1993) Collision avoidance of flying locusts: Steering torques and behaviour. J Exp Biol 183:35–60

Robertson RM, Pearson KG (1982) A preparation for the intracellular analysis of neuronal activity during flight in the locust. J Comp Physiol A 146:311–320

Robertson RM, Pearson KG (1983) Interneurons in the flight system of the locust: distribution, connections and resetting properties. J Comp Neurol 215:33–50

Robertson RM, Reye DN (1992) Wing movements associated with collision-avoidance manoeuvers during flight in the locust, *Locusta migratoria*. J Exp Biol 163:231–258

Rogers SM, Krapp HG, Burrows M, Matheson T (2007) Compensatory plasticity at an identified synapse tunes a visuomotor pathway. J Neurosci 27:4621–4633

Rowell CHF, Pearson KG (1983) Ocellar input to the flight motor system of the locust: structure and function. J Exp Biol 103:265–288

Rowell CHF, Reichert H (1986) Three descending interneurons reporting deviation from course in the locust. II. Physiology. J Comp Physiol A 158:775–794

Santer RD, Simmons PJ, Rind FC (2005) Gliding behaviour elicited by lateral looming stimuli in flying locusts. J Comp Physiol A 191:61–73

Santer RD, Rind FC, Stafford R, Simmons PJ (2006) Role of an identified looming-sensitive neuron in triggering a flying locust's escape. J Neurophysiol 95:3391–3400

Schlotterer GR (1977) Response of the locust descending movement detector neuron to rapidly approaching and withdrawing visual stimuli. Can J Zool 55:1372–1376

Simmons PJ (1980) Connexions between a movement-detecting visual interneurone and flight motoneurones of a locust. J Exp Biol 86:87–97

Simmons PJ, Rind FC (1997) Responses to object approach by a wide field visual neurone, the LGMD2 of the locust: characterization and image cues. J Comp Physiol A 180:203–214

Smith MA, Kohn A (2008) Spatial and temporal scales of neuronal correlation in primary visual cortex. J Neurosci 28:12591–12603

Sun H, Frost BJ (1998) Computation of different optical variables of looming objects in pigeon nucleus rotundus neurons. Nat Neurosci 1:296–303

Vallis LA, McFadyen BJ (2003) Locomotor adjustments for circumvention of an abstacle in the travel path. Exp Brain Res 152:409–414

Vallis L, McFadyen B (2005) Children use different anticipatory control strategies than adults to circumvent an obstacle in the travel path. Exp Brain Res 167:119–127

Verspui R, Gray JR (2009) Visual stimuli induced by self-motion and object-motion modify odour-guided flight of male moths (*Manduca sexta* l.). J Exp Biol 212:3272–3282

Waloff Z (1972) Orientation of flying locusts, *Schistocerca gregaria* (forsk.), in migrating swarms. Bull Ent Res 62:1–72

Yamamoto K, Nakata M, Nakagawa H (2003) Input and output characteristics of collision avoidance behavior in the frog *Rana catesbeiana*. Brain BehavEvol 62:201–211

Yamawaki Y, Toh Y (2009) Responses of descending neurons to looming stimuli in the praying mantis *Tenodera aridifolia*. J Comp Physiol A 195:253–264